IEEE Access
Multidisciplinary | Rapid Review | Open Access Journal

Received April 5, 2021, accepted April 11, 2021, date of publication April 22, 2021, date of current version April 30, 2021.

Digital Object Identifier 10.1109/ACCESS.2021.3074967

Stratification of High-Risk Hypertensive Patients Using Hybrid Heart Rate Variability Features and Boosting Algorithms

DIPEN DEKA[1,2], (Member, IEEE), AND BHABESH DEKA[2], (Senior Member, IEEE)
[1]Department of Instrumentation Engineering, Central Institute of Technology (CIT) at Kokrajhar, Kokrajhar 783370, India
[2]Department of Electronics and Communication Engineering (ECE), School of Engineering, Tezpur University, Tezpur 784028, India

Corresponding author: Bhabesh Deka (bdeka@tezu.ernet.in)

This work was supported by AICTE, India, in providing scholarships under the QIP Scheme, and the Visvesvaraya Ph.D. Scheme in providing necessary equipment and tools for this research.

ABSTRACT Hypertension is a global challenge to the public health which can easily lead to life-threatening vascular diseases unless control measures are adopted. Considering the prevalence of vascular diseases and their fatality, early detection of high-risk patients is an important problem in the present world. Heart rate variability (HRV) analysis can be an effective prognostic tool to identify the characteristics of vulnerable patients, considering its reliability in predicting sudden cardiac deaths. However, challenge lies in identifying tenuous differences in HRV between the low-risk and high-risk patients at the early stage. With this motivation, we propose a hybrid approach based on dual-tree complex wavelet packet transform (DTCWPT) and linear time domain as well as nonlinear analysis of HRV signal to extract multitudinous features. A key issue before the HRV analysis of such patients is the presence of marked amount of ectopic beats, which is addressed by using time-varying auto regressive (TVAR) technique. The features extracted from TVAR edited HRV signals are shortlisted by minimum redundancy maximum relevance algorithm for an efficient classifier modeling. Furthermore in this study, we propose to use cost-sensitive RUSBoost (CS-RUSBoost) algorithm for handling the class imbalance problem of the data. A comparative performance evaluation of CS-RUSBoost with RUSBoost, SMOTEBoost, asymmetric AdaBoost algorithm shows a superior result by CS-RUSBoost with G-mean of 0.9352 and F1 score of 0.9347.

INDEX TERMS Heart rate variability, hypertension, dual-tree complex wavelet packet transform, class imbalance, boosting algorithm.

I. INTRODUCTION

Hypertension (elevated blood pressure) is the most common health problem nowadays with a staggering number of around 1.1 billion people all across the world are victims of it, as per the recent report of world health organization (WHO) [1]. Bad dietary habits, lack of physical activity, and stressed lifestyles are the prime reasons behind the prevalence of hypertension in the present society. Hypertension and vascular pathology compliments each other and thereby aggravates the health of blood vessels. Fatal vascular events such as myocardial infarction, ischemic stroke, hemorrhagic stroke, syncope, etc. are the consequences of persisting vessel pathology. Evidently, lots of research efforts are put into the detection of such conditions, identification of their roots and recognition of the remedial measures [2]–[18]. Heart rate variability (HRV), an established marker of mortality and morbidity has been studied in many works for finding its behavioral change in hypertensive patients and also for predicting the future development of essential hypertension [3], [4], [10], [13]. However the volume of research on characterizing and predicting hypertensive patients who have higher risk of developing acute vascular diseases are very less. In some works besides HRV, ultrasound and echocardiograph based findings are used for predicting the patients vulnerable to acute vascular diseases [5]–[8]. However, HRV is much cheaper, more patient friendly as compared to the above mentioned diagnostic procedures and it could even be assessed from one's home. This can make it a much more attractive diagnostic and prognostic option for analyzing such cardiovascular diseases, provided its reliability is not compromised. Nevertheless, for appropriate prognostic evaluation, cohort study is required. Thanks to Melillo *et al.* [10] for conducting the study on hypertensive patients to discriminate the high-risk hypertensive (HRH) patients from low-risk hypertensive (LRH) patients and providing the data in public domain.

The associate editor coordinating the review of this manuscript and approving it for publication was Nilanjan Dey.

This database is available in PhysioNet repository as ''Smart Health for Assessing the Risk of Events via ECG (SHAREE) database''. Using the data, Rajput *et al.* [11] have computed signal fractal dimension and log energy entropy from the wavelet coefficients of ECG signals. For that purpose, they decomposed the ECG signals into 6 wavelet sub-bands using optimal orthogonal wavelet filter bank. Their classification result shows 100% accuracy in separating the low risk and high risk patients. In another study, Soh *et al.* [12] merged both the LRH and HRH patients as hypertension group and discriminated it from normal subjects' group by extracting nonlinear features from the intrinsic mode functions of ECG signals. They achieved an accuracy of 97.70% using k-nearest neighbor (KNN) classifier.

Besides these ECG based studies, many researchers have used HRV signals to detect and predict hypertension, stroke, sudden cardiac death (SCD), and different coronary artery diseases (CADs) [10], [13]–[17], [19], [20]. In a study by Lan *et al.* [13], linear time domain parameters such as standard deviation of normal to normal intervals (SDNN), mean interbeat interval (MeanRR), and root mean squared value of successive differences between normal to normal intervals (RMSSD), and spectral power parameters, namely normalized low frequency power (LFnu), normalized high frequency power (HFnu), and LF/HF are computed from the photoplethysmogram (PPG) based HRV data. They concluded that SDNN has the highest discriminative power to separate the normal and hypertensive subjects. In [14], the spectral powers are calculated by both fast Fourier transform and autoregressive model fitting methods. Additionally, they obtained the traditional time domain parameters and the nonlinear parameters (Poincare plot based features, approximate entropy, sample entropy) to classify the normal, hypertension and CADs. They achieved the best accuracy of 96.67% by using support vector machine (SVM) classifier. In [15], scaling property of HRV signal is used to detect the subjects vulnerable to SCD from a random samples of elderly subjects. Authors found short-term scaling exponents (α_1) to be more effective than power-law slope and SDNN in distinguishing the normal subjects and SCD subjects. In [16], authors used smoothed pseudo Wigner-Ville distribution method to undergo time-frequency analysis of HRV signals besides the linear and nonlinear methods for extracting the discriminative features. They found that the multilayer perceptron (MLP) classifier edges over the KNN classifier in predicting SCD prone subjects with accuracy of 99.73%, 96.52%, 90.37% and 83.96% for the first, second, third and fourth one-minute intervals before the onset of SCD event. In [17], authors performed automated prediction of SCD using recurrence quantification analysis and Kolmogorov complexity parameters extracted from HRV signals. They obtained better performance (Accuracy: 86.8%) from PNN and KNN as compared to SVM classifier. In a work on the prediction of ischemic stroke, authors [19] concluded that the subjects with familial records of premature heart attack and depressed HRV are more prone to focal coronary atherosclerosis as well as vascular death. Binici *et al.* [20] conducted an HRV based study on middle-aged and elderly white subjects to examine the link between reduced HRV and increased risk of stroke. They found that SDNN value for subjects prone to stroke is significantly lower ($p = 0.004$) as compared to non risky subjects at nighttime. In [21], Kampouraki *et al.* have computed statistical time-domain features, local linear prediction and standard deviation of detail coefficients from wavelet analysis to distinguish the normal subjects from subjects suffering from CAD using SVM classifier. In [10], Melillo *et al.* extracted multiple linear as well as nonlinear parameters from HRV signals of hypertensive patients and used classifiers namely Adaboost, classification and regression tree (CART) 4.5, SVM, MLP, naive Bayes and random forest (RF) classifiers to conduct a comparative analysis. They achieved best performance from random forest classifier with sensitivity of 71.4% and specificity of 87.8% in predicting the high-risk patients.

From the literature study, it is apparent that some of the key issues in HRV analysis for detecting the high-risk hypertensive patients (vulnerable to CAD, stroke, SCD, etc.) are yet to be addressed in more details to avoid misleading analysis. Firstly, such patients' data contain substantial amount of ectopic as well as missed beats. So, they should be handled appropriately for reliable analysis. Secondly, in case of wavelet based time-frequency analysis, level of decomposition and sampling frequency should be chosen in such a way that LF and HF components of HRV should not overlap. Thirdly, often classification of the positive group (with diseased condition) are scarce as compared to the control group. So, the issue of class imbalance should be addressed with care while performing the classification task. With these objectives, we have first used time varying autoregressive (TVAR) model to treat the ectopic/missed beats and then conducted hybrid HRV analysis based on the results from dual tree complex wavelet packet transform (DTCWPT)-, statistical time-, as well as nonlinear analysis. Finally, we have tested 4 different boosting algorithms for addressing cost-imbalance issue to draw out the best classification performance.

The rest of the paper is structured as follows. Section II briefs the methodology adopted to carry out the work and describes the theoretical background of the methods used. In Section III, we demonstrate the simulation results and provided their discussion. Finally, we conclude the paper by highlighting the key findings and future research direction in Section IV.

II. MATERIALS AND METHODS

The flowchart of the proposed methodology is portrayed in Fig. 1. In the subsequent sub-sections, we describe the theoretical background of the methods used to implement the work.

A. DATA

We acquire the ''Smart Health for Assessing the Risk of Events via ECG (SHAREE) database'' [10], [22] from the PhysioNet website to carry out the proposed work. This data

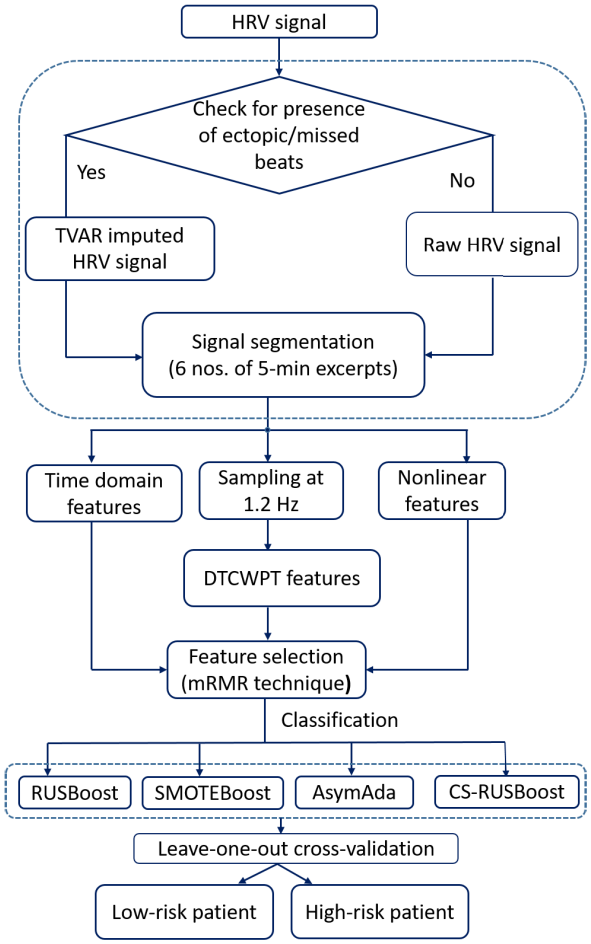

FIGURE 1. Flowchart of the proposed methodology.

contains 24-hr ECG Holter recordings of 139 hypertensive patients. The ECG signals were sampled at 128 Hz with an 8-bit ADC. Out of these patients, 49 are female and 90 are male with ages $\geq$ 55 years. After taking the recordings, they were followed up for another 12 months to record any vascular events. In the follow-up period, 17 patients experienced such vascular events with 11 myocardial infarctions, 3 strokes and 3 syncopal events. These 17 patients are regarded as HRH patients, while the others as LRH patients. It is to underscore here that both the LRH and HRH patient's data used for this predictive study are of hypertensive patients with no previous records of any vascular events. However, later on some developed vascular events, who are labelled as HRH patients. Furthermore, the patients were also tested by a cardiac and carotid ultrasonograph to examine the left ventricular mass and intima media thickness. Due to the presence of large ($>$ 40%) no. of ectopic/missed beats, 26 subjects' data from LRH group and 2 subjects' data from HRH group are excluded from our study.

B. DATA PREPROCESSING

The acquired data has already surpassed basic preprocessing steps like sampling and the conversion of ECG signals into RR intervals form. So, we have first checked for the presence of any ectopic and missed beats by using a proposed HRV data (RR intervals data) correction algorithm. According to the algorithm, any RR intervals exceeding 2 sec are considered as missed beat events. In the next step, we calculated the median values of the RR intervals for a data length of 2 min. We have chosen median value (Med) instead of mean, as in case of the presence of many ectopic beats, mean value will be highly deviated from the actual mean of the signal, while median value is quite robust to outliers due to missed/ectopic beats. Further, 2 min of window time is chosen, as for the larger or whole length of the signal, RR intervals may change drastically. So this will avoid fallacious detection of ectopic beats. Over the 2 min window, any RR intervals exceeding $1.6 \times Med_i$ or lesser than $0.65 \times Med_i$ are to be replaced by a value obtained from time varying autoregressive (TVAR) model fitting. This step will eliminate especially any forms of exceptionally small/large beats such as, r beats: R on T (fiducial points of ECG) premature ventricular contraction, S beats: supraventricular premature beat, V beats: premature ventricular contraction, F beats: fusion of ventricular and normal beats, and Q beats: unknown beats. Afterwards, to remove atrial/ventricular premature/ectopic beats with small jumps, our algorithm compares every consecutive RR intervals. For this purpose, we set a high threshold of $1.18 \times RR_{i-1}$ and a low threshold of $0.86 \times RR_{i-1}$, after studying the RR intervals data variations rigorously. Here, RR_{i-1} indicates the previous RR interval data point with which the present RR interval data point is compared. The RR intervals data crossing the low/high threshold are to be replaced. To replace these RR intervals data points, different techniques like linear interpolation, nonlinear interpolation (e.g. squared, cubic spline, pchip), artificial neural network (ANN) based imputation, AR based interpolation, etc. are available. However, due to higher computational cost and dynamical complexity of RR interval series, we have dropped the ANN based imputation technique for this study.

To illustrate these issues properly, we have demonstrated a few types of outliers in Figs. 2 and 3. Although outliers of different forms can be edited using linear and nonlinear interpolation techniques, they have some limitations. For instance, considering a missed beat event of around 3 (or may be more) sec due to any actual cardiac premature events or electrode connectivity issue, if the RR interval before this event and after this event are equal (say, 0.850 sec), a linear interpolation technique will generate 3/0.850$\sim$ 4 additional RR intervals in between with the same RR interval (0.850 sec). The results of imputation for such cases are presented in Section III. This will lead to incorrect statistical measures (SDNN, RMSSD, SDANN, etc.) as well as faulty permutation entropy, scaling exponent, to name a few. However, under such circumstance, nonlinear interpolation technique will perform well. But, if the outliers are located at the beginning/end of the segment, nonlinear interpolation technique will provide wild variations.

So we have adopted time-varying AR (TVAR) model to fit the data with an aim to overcome the above mentioned issues

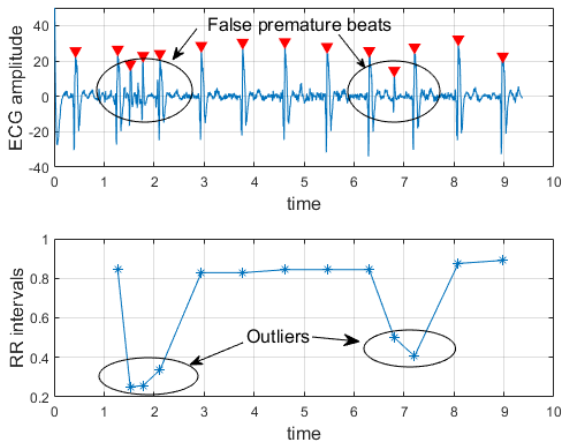

FIGURE 2. Erroneous HRV signal due to the presence of false beats.

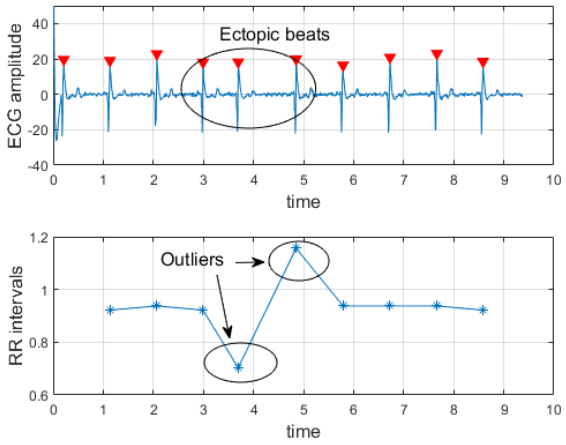

FIGURE 3. Erroneous HRV signal due to the presence of ectopic beats.

of parallel methods. The non-stationary behaviour of HRV signal led us to avoid the regular AR technique. To the best of our knowledge, TVAR model is not used for imputation purpose earlier. We have utilized the idea of forgetting factor and previous coefficients as used by Bianchi *et al.* [23] to predict the replaceable data point. However, we have modified the method by using the coefficients based on the minimization of forward and backward prediction errors. In our method, firstly all the discarded RR intervals are replaced by NaN (not a number) on MATLAB environment. The forward and backward prediction errors are computed from the errorfree RR interval data points and their index information. The forward prediction error ($e_{f,p}(n)$) is given by [24]

$$\begin{aligned} e_{f,p}(n) &= RR_{k_i}(n) - \widetilde{RR}_{k_i}(n) \\ &= \sum_{i=0}^{p} w^{k_p - k_i} a_{k_i,p} RR_k(n - k_i) \end{aligned} \tag{1}$$

where $RR_{k_i}(n)$ is the series having p nos. of errorfree data points and the indices are given by k_i, and p is the model order obtained using AIC. In this case, the past samples $RR_{k_i}(n-k_i)$ are only the past errorfree RR intervals and w is the forgetting factor (here, $w = 0.95$) whose influence decreases with the increase in time separation from the current sample. The backward prediction error ($e_{b,p}(n)$) that takes place while predicting the present sample from its future samples is given by

$$\begin{aligned} e_{b,p}(n) &= RR_{k_i}(n - k_p) - \widetilde{RR}_{k_i}(n - k_p) \\ &= \sum_{i=0}^{p} w^{k_p - k_i} * a_{p,p-k_i} RR_{k_i}(n - k_i) \end{aligned} \tag{2}$$

The sum of the squares of both $e_{f,p}(n)$ and $e_{b,p}(n)$ are then minimized according to Burg's recursion algorithm to obtain the AR coefficients at the indices having errorfree RR intervals. The coefficients for both backward and forward prediction and their sample values are used to determine the missed RR intervals. Further details about Burg's recursion algorithm can be found in [25]. After getting the filled RR interval series, they are segmented into 6 excerpts of 5 min length for feature extractions.

C. FEATURE EXTRACTION

1) TIME DOMAIN PARAMETERS

Apart from the traditional time domain HRV parameters such as, SDNN, standard deviation of differences of RR intervals (SDDER), some unconventional time domain parameters, namely, the standard deviation of second order differences of RR intervals (SDSOD), median absolute deviation of differences of RR intervals (MADDER), median absolute deviation (MAD), and Hjorth's mobility are computed in this study to find if they are able to discriminate the HRV of LRH and HRH patients. These parameters are obtained using the 5 min RR interval segments of all the subjects. A brief definition and the mathematical expressions of these functions are given below:

SDNN is a measure of the standard deviation of normal to normal interbeat intervals of 5 min segments [26].

$$\text{SDNN} = \sqrt{\frac{1}{N}\sum_{i=1}^{N}\left[RR(i) - \overline{RR}\right]^2} \tag{3}$$

where N is the total no. of samples in the 5 min segment/excerpt and $RR(i)$ is the ith RR interval.

SDDER provides the standard deviation of the differences in RR intervals. It indicates the extent of variability of RR intervals at one step higher order.

$$\text{SDDER} = \sqrt{\frac{1}{N-1}\sum_{i=1}^{N-1}\left[DRR(i) - \overline{DRR}\right]^2} \tag{4}$$

where $DRR(i)$ is the first order derivative of $RR(i)$ series and $\overline{DRR}$ is the mean of $DRR(i)$.

SDSOD is another term indicating the higher order variations in RR interval series. It provides the standard deviation of second order differences of RR interval series. It is found to be very effective in discriminating the HRV of meditative and pre-meditative states [27], which led us to test its discriminative power in separating the HRV of LRH and HRH subjects.

$$\text{SDSOD} = \sqrt{\frac{1}{N-2}\sum_{i=1}^{N-2}\left[\text{SDDER}(i) - \overline{\text{SDDER}}\right]^2} \tag{5}$$

MAD determines the median value of the absolute deviations of RR intervals from its mean value. Then obtain its average value.

$$\text{MAD} = \text{median}(\left|RR(i) - \overline{RR}\right|) \tag{6}$$

MADDER is the median value of the first order derivative of RR interval series.

$$\text{MADDER} = \text{median}(\left|DRR(i) - \overline{DRR}\right|) \tag{7}$$

Mobility is a parameter introduced by Hjorth [28] to study the complex fluctuation in electroencephalogram. It can be defined here as the ratio of the activity of the differences of RR interval series to the activity of the RR interval series.

$$\text{Mobility} = \frac{\text{SDDER}}{\text{SDNN}} \tag{8}$$

2) DUAL-TREE COMPLEX WAVELET PACKET TRANSFORM (DTCWPT) BASED TIME-FREQUENCY ANALYSIS

Due to several significant advantages, like shift invariance property, highly aliasing free and non oscillatory (unlike the positive and negative oscillations at the singular/transient points in case of real wavelets) behaviour, complex wavelets like DTCWT and DTCWPT could provide more accurate time-frequency (TF) analysis. Though, continuous wavelet transform (CWT) also possess these advantages, there is high computational burden associated with it. On that ground, both DTCWT and DTCWPT offers computational efficiency with complexity order of only $2N$ and $N \log_2 N$ respectively. Here, even though DTCWT is efficient for simultaneous TF analysis, it has lower frequency resolution since it decomposes only the approximate coefficients of the signal. Especially for HRV analysis, to meet up to frequency bands (0.04-0.15 Hz, and 0.15-0.4 Hz), higher frequency resolution is required. Having this issue, DTCWPT is more suitable for our analysis, with its high frequency resolution as it decomposes also the detail coefficients progressively [29].

Delving into the basic theory, DTCWPT uses two branches of filter banks (FBs) like DTCWT; one of them is called real tree and the other one as imaginary tree. If the wavelet functions corresponding to the real and imaginary trees are given by $\psi^{Re}(t)$ and $\psi^{Im}(t)$ respectively and similarly, $\phi^{Re}(t)$ and $\phi^{Im}(t)$ are the scaling functions for real and imaginary trees, their mathematical expressions are given by:

$$\begin{aligned}\psi^{Re}(t) &= \sqrt{2}\sum_n h_1^{Re}(n)\psi(2t-n)\\ \psi^{Im}(t) &= \sqrt{2}\sum_n h_1^{Im}(n)\psi(2t-n)\end{aligned} \tag{9}$$

where $h_1^{Re}(n)$ and $h_1^{Im}(n)$ are the high pass filters of real and imaginary trees respectively.

$$\begin{aligned}\phi^{Re}(t) &= \sqrt{2}\sum_n h_0^{Re}(n)\phi(2t-n)\\ \phi^{Im}(t) &= \sqrt{2}\sum_n h_0^{Im}(n)\phi(2t-n)\end{aligned} \tag{10}$$

where $h_0^{Re}(n)$ and $h_0^{Im}(n)$ are the low pass filters of real and imaginary trees respectively. Using (9) and (10), the complex wavelet and scaling functions can be obtained as: $\psi^C(t) = \psi^{Re}(t) + i\psi^{Im}(t)$ and $\phi^C(t) = \phi^{Re}(t) + i\phi^{Im}(t)$. The real and imaginary wavelet functions are chosen in a way that they nearly forms Hilbert transform pair to achieve analyticity, given by $\psi^{Im}(t) \approx H[\psi^{Re}(t)]$. For real orthonormal wavelet functions, analyticity can be achieved if the following condition is satisfied

$$h_0^{Im}(n) = h_0^{Re}(n - 0.5) \tag{11}$$

To have the decomposition of detail coefficients, FB pairs are introduced into the high frequency branch. To preserve Hilbert transform property, the same extension filters $(f_0(n), f_1(n)$, etc.) should be used to both FBs of both the trees. The quadratic-shift filters in the imaginary tree differs from that in the real tree by the relation: $h_i^2(n) = h_i^1(n-1)$, and $h_i^{Im}(n)$ may be different from $h_i^{Re}(n)$ for $i \in \{0, 1\}$. A representative analysis filter bank for 2-stage DTCWPT is demonstrated in Fig. 4. In case of 4-stage DTCWPT, simply two more level of decomposition takes place which will result into 16 real coefficients and 16 imaginary coefficients. For this study, we have chosen sampling frequency of 1.2 Hz ($\geq$ 2× (peak frequency)) and 4th level of decomposition using db6 wavelet to extract the sub-band coefficients. From these decomposed coefficients, the signals corresponding to the individual sub-bands can be reconstructed by treating other sub-band coefficients as zero. This yields 16 sub-bands, out of which some of the sub-bands (nodes: 9, 10, 11, 12) are out our interest as they exceeds the frequency range of HRV signal. These reconstructed sub-bands maintain the same length as that of the signal, which adds some advantage for the measure of some length constraint features. We extract features namely, Shannon entropy (ShEn), L2 norm entropy (NormEn), sample entropy (SampEn), crest factor (CF), sum of absolute variations (SumVar), and root mean squared value of the coefficients (RMS) from the sub-bands. Their mathematical definitions are given below:

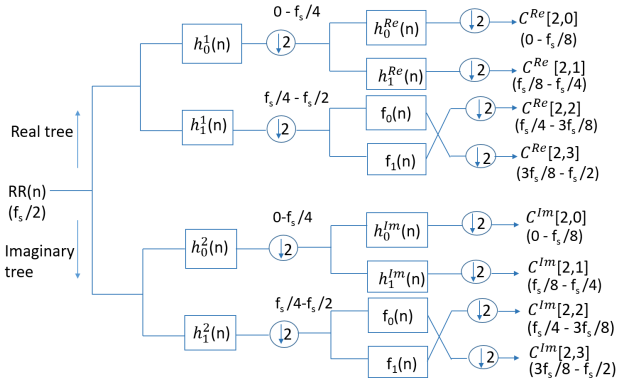

FIGURE 4. Analysis filter banks of 2-stage DTCWPT.

ShEn: It calculates the Shannon entropy from the distribution of the squares of the coefficients of a sub-band.

$$\text{ShEn} = -\sum_{i=1}^{N}[C(i)]^2 \log[C(i)]^2 \tag{12}$$

where $C(i)$ are the coefficients of length N in a sub-band.

NormEn: This parameter provides L2 norm entropy of the coefficients of a reconstructed sub-band.

$$\text{NormEn} = \sum_{i=1}^{N} |C(i)|^2 \tag{13}$$

SampEn: It provides the complexity of a time series by evaluating the changes in the Chebyshev distance between embedded vectors with the increase in embedding dimension. It is given by

$$\text{SampEn} = -\log \frac{N_{m+1}}{N_m} \tag{14}$$

where N_{m+1} and N_m are the no. of pairs of embedded vectors with their chebyshev distance less than a specified tolerance limit in $m+1$ and m dimensional phase space respectively.

CF: It is the ratio of peak magnitude of the coefficients to the rms value of the coefficients in a sub-band.

$$\text{CF} = \max(C(i))/\text{rms}(C(i)) \tag{15}$$

SumVar: It measures the sum of the absolute differences between consecutive magnitudes of the coefficients.

$$\text{SumVar} = \sum_{i=1}^{N-1} |C(i+1) - C(i)| \tag{16}$$

RMS: It provides the rms magnitude of the coefficients in a band.

$$\text{RMS} = \sqrt{\frac{1}{N}\sum_{i=1}^{N} C(i)^2} \tag{17}$$

3) MULTISCALE ENTROPY ANALYSIS BASED ON DISPERSION ENTROPY

Multiscale entropy as introduced by Costa *et al.* [30] is having increased importance in analyzing complexity of a signal, as true complexity of a process may not be ascertained from single scale. The concept of multiscale entropy is brought into several different information descriptors. Rostagi and Azami [31] developed an entropy named dispersion entropy to address mainly issue of limited sensitivity of permutation entropy. Unlike permutation entropy in which only ordinal pattern is considered instead of amplitudes, dispersion entropy is more sensitive to the variation in magnitude and robust to the noise/outliers at the same. For that matter, to evaluate the heart rate generative process in case of LRH and HRH patients, we have used multiscale dispersion entropy (MDE). We have computed the values for scales from 1 to 5 ($\in \mathbb{Z}$). For more theoretical background, readers can refer to [31].

D. FEATURE SELECTION

After extracting all the features, it is essential to find out the discriminative as well as the non-redundant features out of the whole set. This is aimed at improving both the computational efficiency and classification results. We have employed mutual information based minimum redundancy maximum relevance (mRMR) technique [32] for feature selection.

E. CLASSIFICATION AND CROSS-VALIDATION

Considering the skewed class distribution of our data, we propose cost-sensitive RUSBoost (CS-RUSBoost) in addition to regular RUSBoost, SMOTEBoost, and asymmetric adaboost to evaluate their effectiveness for the given data. RUSBoost uses random undersampling technique to reduce the majority class observation size to minority class [33], while SMOTEBoost increases the minority class size by using intelligent oversampling technique [34]. Literature show that RUSBoost can produce equivalent result to that of SMOTEBoost, besides being computationally more efficient as compared to SMOTEBoost. On the contrary, the asymmetric Adaboost [35] is a cost-sensitive technique which applies different cost to false positive and false negative outcomes depending on the class of importance. Asymmetric Adaboost (AsymAda) can highly elevate the detection of important class at the minor cost of few more misclassifications in less important class. In this work we have blended the principle of RUSBoost and asymmetric costing (higher cost on false negative) to yield higher accuracy in detecting the high-risk hypertensive patient at lower computational burden.

The classifier performance is cross-validated using leave-one-subject-out cross-validation (LOOCV) technique since it provides unbiased evaluation of the classifier. This technique also ensures that all the segments from a single subject be either on the training or test set, thereby avoids the possibility of overfitting.

III. RESULTS AND DISCUSSION

We have performed the simulation works on MATLAB R2018a environment using a computer configured with Intel (R) core (TM): i7 processor, 2.40 GHz clock speed and 4 GB of memory.

A. DATA PREPROCESSING

We first demonstrate the outputs of three ectopic/missed beats imputation techniques in Fig. 5. For this, we have arbitrarily chosen an annotated HRV segment from a subject (16265) belonging to the ''The MIT-BIH Normal Sinus Rhythm Database'' of PhysioNet repository [22]. While choosing the segment, we have just ensured that it does not contain any ectopic beats, which is graphically shown in Fig. 5(a). The reason behind the use of real-life signal is to conserve the typical dynamical behaviour of HRV; while, annotated segment (by expert) eradicates the chances of false assumption about normal/ectopic beats. Subsequently, we have synthetically replaced some normal beats by premature ventricular contraction (PVC) beats with compensatory pause at beat positions 1, 2, 8, 9, 10 and 11; premature atrial contraction (PAC) beat along with its non-compensatory pause at positions 12 and 13, a non-compensatory S beats at positions 24, 25 and an outlier due to missed beat at position 38 (Fig. 5(b)). It is evident from Fig. 5(c) that our algorithm has

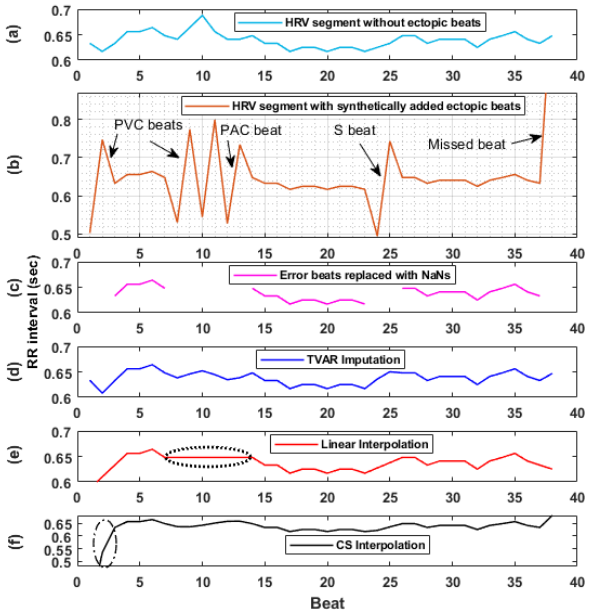

FIGURE 5. (a). An HRV segment without ectopic beats (Subject: 16265) [22], (b). The same HRV segment, whose some of the beats are replaced with PVC, PAC, S and missed beats, (c). Detection of ectopic/missed beats by proposed method and their replacement by NaNs, (d). Imputed HRV segment with TVAR technique, (e). Imputed HRV segment with linear interpolation technique, (f). Imputed HRV segment with CS interpolation technique.

efficiently detected these erroneous beats and replace them by NaNs as discussed in Section II-B. Generally, for an HRV signal with ectopic beats anywhere in between the segment but not on the edges (beginning/end) are almost decently imputed by linear- and cubic spline (CS) interpolation. However, if the ectopic beats are on the edges, cubic spline fails miserably (Fig. 5(f)). The imputed values for these beats as highlighted by dash-dotted ellipse are found to be way larger/smaller than the RR intervals around it. Similarly, if the RR interval values before the gap (beat number 7) and after the gap (beat number 14) are same, then linear interpolation technique returns the same value (beat numbers 8 to 13) as portrayed by dotted ellipse in Fig. 5(e). This leads to an underestimation of HRV and its various measures, be it time, frequency or nonlinear methods based. However, under this particular case, CS interpolation technique works well, provided the ectopic beats are not on the edges. Furthermore, it can be observed that for the S beat, the performance of these techniques are comparable as, these two beats are neither surrounded by beats having same value, nor they are on the edges of the segment. Therefore, both the linear and CS interpolation methods have some desirability and pitfalls. Under all such cases, TVAR based imputation technique is found to be closely following the original HRV signal as compared to these traditional methods of interpolation as illustrated by Fig. 5(d). To quantify the performance of these data imputation techniques, we have determined the mean squared error (MSE) from the original HRV segment and the imputed outcomes. The MSE of TVAR ($\text{MSE}_{\text{TVAR}} = 2.2 \times 10^{-4}$) based imputation technique is found to be ∼2 times lesser than MSE of linear interpolation technique ($\text{MSE}_{\text{LI}} = 4.58 \times 10^{-4}$) and ∼15 times lesser than MSE of CS interpolation ($\text{MSE}_{\text{CS}} = 0.0031$) technique for the chosen HRV segment of length 38 with 11 erroneous data points. It indicates the efficacy of TVAR based method for replacement of ectopic beats in HRV signal. On a nutshell, TVAR model based method avoids the aberrantly high variations as well as eliminates the possibility of getting uncharacteristic zero variation as demonstrated by dotted ellipse in Fig. 5(e).

B. FEATURE EXTRACTION AND THEIR ANALYSIS

From the TVAR imputed (wherever required) HRV signal, a total of 78 features are extracted. Out of this whole feature set, 66 features are extracted using DTCWPT based analysis from its 11 sub-bands excluding the sub-bands corresponding to the nodes 1, 9, 10, 11, 12, as the first sub-band contains both the ultra low and very low frequency components, while the other 4 sub-bands are out of the frequency range of HRV signal; remaining 12 features are extracted directly from the HRV signal using statistical and multiscale entropy based analysis. In this study, 576 (96 × 6) HRV segments are taken from LRH patients and 90 (15 × 6) segments from HRH patients with six segments from each subject; this forms a feature matrix of size 666 × 78. To draw the strong features, they are ranked using mRMR technique, whose result is presented in Fig. 6. The figure shows feature importance scores (S) of only top 30 features due to space constraints and also due to the diminutive S scores from rank-19 onwards. From these features, we have selected the top 12 features to train the classifiers.

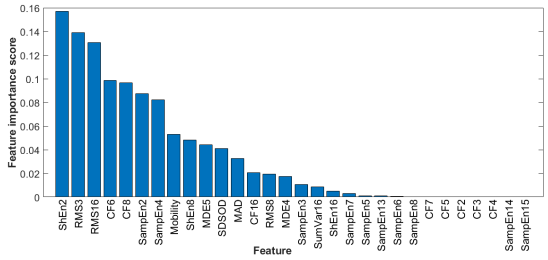

FIGURE 6. Feature importance scores based on mRMR technique.

The variations of these shortlisted features for the LRH and HRH patients are portrayed by the box-plots in Fig. 7. The red line in the blue boxes represent the median value of a feature, while the whiskers indicates their lowest and highest values. Furthermore, some outliers can be observed in the features of these plots, indicated by red '+' mark. Some of the features are denominated with subscripts (e.g., ShEn_2), where the subscript indicates the node number of the DTCWPT decomposition tree. On observing the box plots, it can be ascertained that the selected features are able to distinguish the LRH and HRH patients considerably well. However, minor overlapping region exists between the LRH and HRH groups for all the features. Interestingly, all the entropy parameters

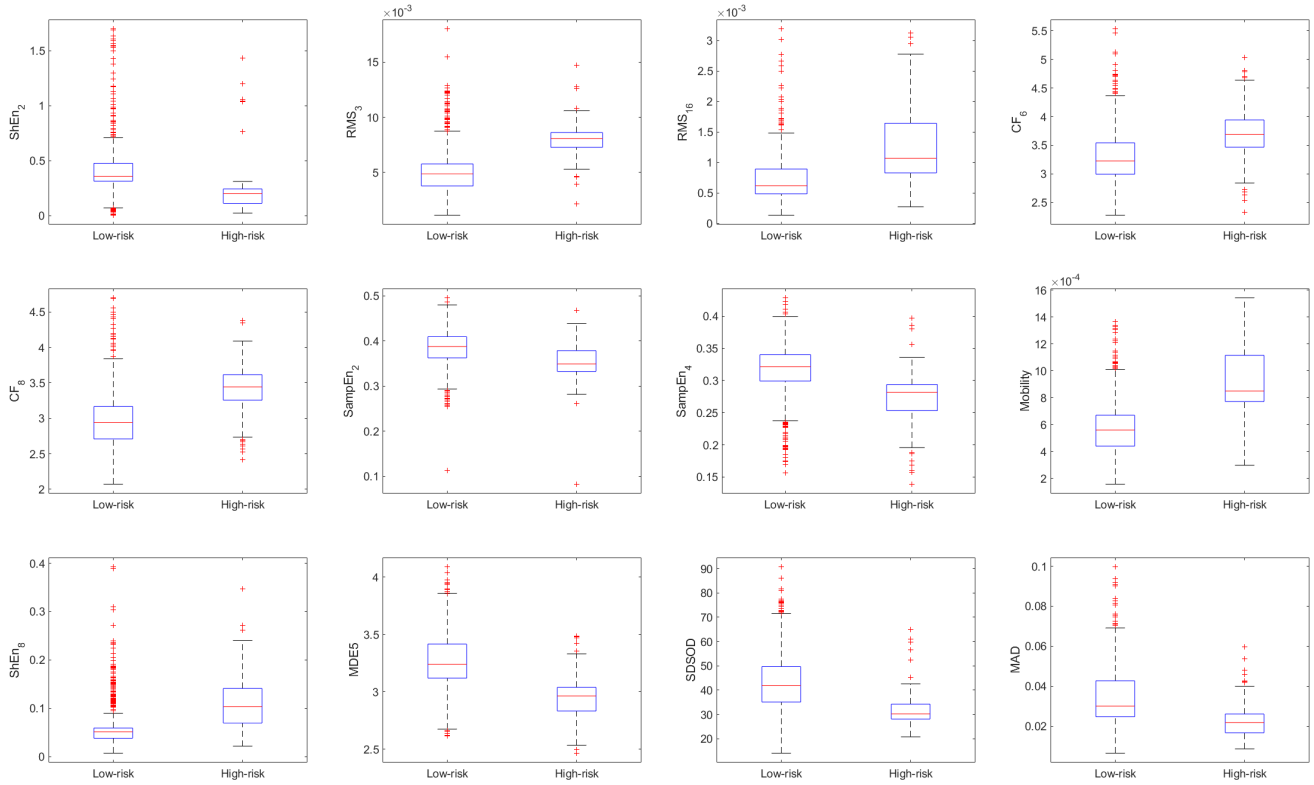

FIGURE 7. Box-plot of the shortlisted features extracted from the HRV signal of low-risk and high risk hypertensive patients.

except, $ShEn_8$ are having lower magnitude in HRH patients as compared to the LRH patients. It can be observed that these entropy parameters ($ShEn_2$, $SampEn_2$, $ShEn_4$) are extracted from DTCWPT nodes corresponding to the LF components, whereas $ShEn_8$ is extracted from the corresponding HF component. This reflects that at LF region, the HRH patients have lesser spectral modulation as compared to LRH patients and the reverse is the case in HF region. This reveals variation of the activity of autonomic nervous system in LRH and HRH patients. Further, MDE5, i.e., the dispersion entropy obtained directly from the HRV signal at scale 5 is also lesser in HRH patients as compared to the LRH patients. This confirms that that dynamical complexity gets reduced in HRH patients. On zooming into the spectral behaviour of the HRV signal of HRH and LRH patients, we observe that under LF region (nodes 2, 3 and 4), the degree of fluctuation is much reduced in HRH patients as demonstrated in Fig. 8. The amplitude of these LF components lie in between ± 0.01 for HRH patients, whereas for LRH patients, the amplitudes are around 5 times larger. On the other hand, under HF region, the amplitudes are within similar range for both types of patients; however, their energies (amplitudes) are concentrated in few patches in case of LRH patients, whereas they are more distributed in case of HRH patients as demonstrated by nodes 6, 7, 8, 14, and 16 in Fig. 9. This leads to an increased entropy ($ShEn_8$) and RMS (RMS_{16}) values at HF region in HRH patients, as demonstrated in Fig. 8. It is to be mentioned here that HRV analysis based on DTCWT or DWT includes components from both LF and HF regions in some of their nodes because of their limited frequency resolution, which makes it impossible to provide such detailed analysis specifically at LF/HF regions as given by DTCWPT analysis.

C. CLASSIFICATION

As the ratio of negative class (LRH) size to the positive class (HRH) size is more than 6, regular classification technique will be unsuitable for their inclined results towards the larger class. Obviously, the classifier with more training on one kind of data will label anything similar to that data as that class only. Further, as overall accuracy can not provide the real performance of the classifier at least in terms of the positive class, we have obtained the receiver operating characteristic (ROC), whose result is portrayed in Fig. 10. It shows the variation in true positive rate vs. false positive rate for the 4 classifiers used to deal with the class imbalance issue as discussed in Section II-E. It can be observed that CS-RUSBoost classifier provides the highest area under the ROC curve (AUC) as compared to the other 3 classifiers. These results are obtained by using the decision tree learner C4.5 as the base learner in all of these classifiers. In CS-RUSBoost algorithm, we have followed the weight updation rule and initial weights as used in ADAC2 algorithm [36]. Further, cost ratio ($c = \frac{C_{FP}}{C_{FP}+C_{FN}}$) is manually selected after carrying out a comparative analysis by using different ratios. Finally, we have assigned a higher cost of factor 2 to FN and 1 to FP, while TP and TN are assigned zero values. A comparison of the performance evaluation based on precision, recall, geometric mean (G-mean), F1 score,

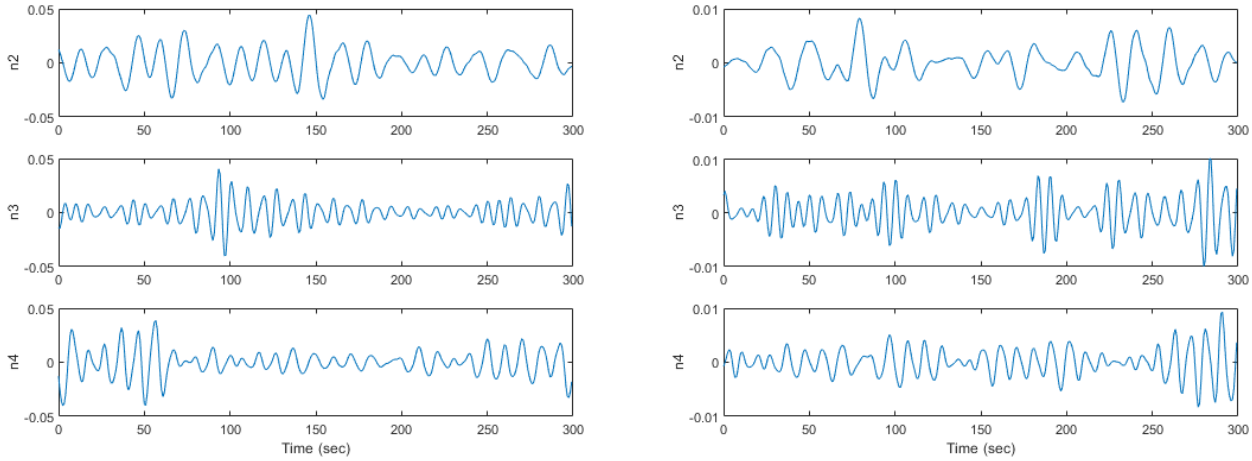

FIGURE 8. Reconstructed nodes corresponding to LF components of the HRV signal of LRH (left) and HRH (right) patients.

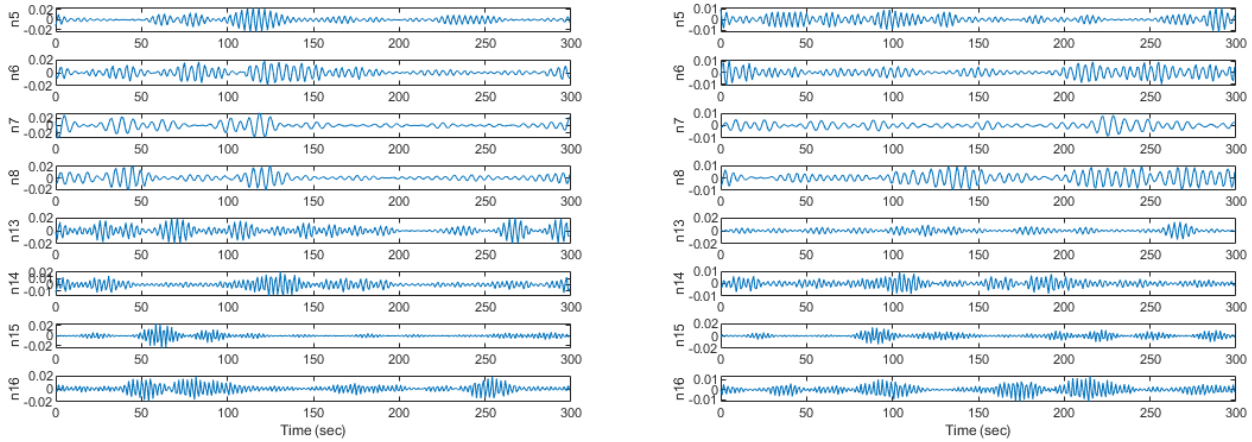

FIGURE 9. Reconstructed nodes corresponding to HF components of the HRV signal of LRH (left) and HRH (right) patients.

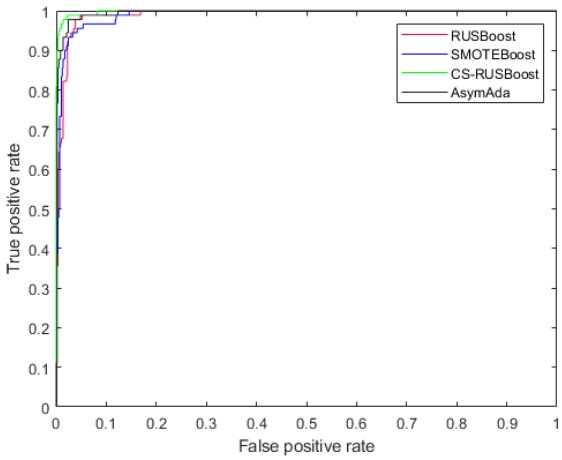

FIGURE 10. Comparison of ROC Curves for 4 different boosting algorithms cross-validated by LOOCV.

and AUC is demonstrated in Table 1. As initially we grew 200 trees, which provided the classification performance as shown in table 1, afterwards we have checked the performance by reducing the no. of trees to enhance the computational efficiency. A comparison of G-mean and F1 scores, false positive rate (FPR) and false negative rates (FNR) against the no. of trees for CS-RUSBoost classifier are shown in Fig. 11. From this, we observe that performance indices do not change remarkably beyond $\sim$ 15 trees and instead it degrades marginally beyond 250 trees. So, for this study we finally selected 20 trees in our model, which provides computational efficiency of approximately 2 times to that with 200 trees. The proposed model with 20 trees has misclassified just three observations of negative class, while for positive class the detection performance remains the same, whose result is shown in Table 2.

TABLE 1. Comparison of performance of the classifiers.

Classifier	Sensitivity (%)	Specificity (%)	G-mean	F1 score	AUC
RUSBoost	90.00	98.09	0.89	0.89	0.99
SMOTEBoost	91.11	97.74	0.886	0.88	0.989
AsymAda	95.55	98.78	0.940	0.939	0.995
CS-RUSBoost	96.67	98.95	0.951	0.951	0.998

TABLE 2. Performance indices of the proposed classifier model.

Classifier	G-mean	F1 score	FPR (%)	FNR (%)	Computational time (sec)
CS-RUSBoost	0.9352	0.9347	1.56	3.37	4.56 sec

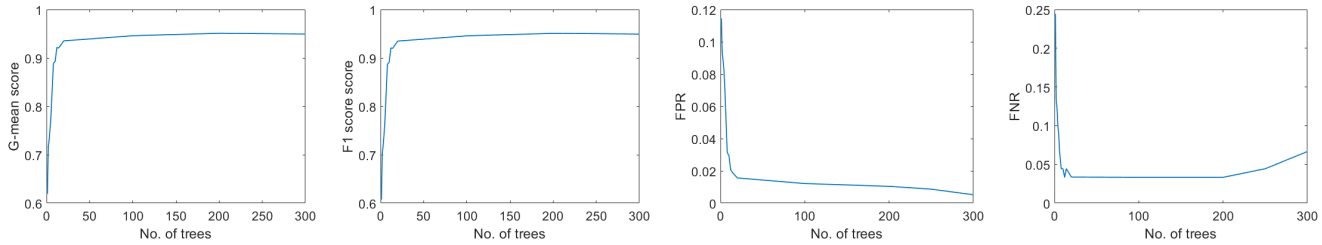

FIGURE 11. Variation of performance indices with the no. of trees.

D. COMPARISON WITH THE RELEVANT WORKS

Literature search shows that very few works have studied on predicting/classifying HRH patients. In [10], Melillo *et al.* have presented a prediction system based on multiple classifiers and HRV features extracted from time, frequency, and nonlinear analysis. They achieved an accuracy of 85.7%, sensitivity of 71.4% and specificity of 87.8% using RF classifier. In [11], Rajput *et al.* have rather used ECG signal to discriminate the LRH and HRH groups based on two parameters namely the fractal dimension and log energy entropy. Their result demonstrates an accuracy of 100% in distinguishing the two groups. In another study, Soh *et al.* [12] have also performed an ECG based classification work by considering both the LRH and HRH patients as hypertension group and normal subjects' group as the control group. By using KNN classifier, they obtained an accuracy of 97.70%. Although, marginally higher accuracy is observed in [11], [12] as compared to our proposed method, they employed ECG signal for their analysis; whereas we have used HRV signal, which has certain advantages. It is worthwhile to mention that HRV signal is much easier to acquire, suitable for telemetry due to its very small bandwidth, very cost effective and more patient friendly, given the fact that it can be derived from photoplethysmogram or any pulse sensors also, whereas acquisition of ECG needs multiple electrodes and robust filtering circuitry. While, considering the methodologies of the existing related works, the issue of multitudes of ectopic beats present either in ECG/HRV signals are not examined. Therefore, we have intended to provide a robust preprocessing method before going for HRV analysis in order to avoid misleading results. Furthermore, the issue of skewed class distribution is also not taken into consideration in these related works. Addressing these factors, our proposed methodology provides an sensitivity of 96.67%, specificity of 98.95%, G-mean score of 0.951, F1 score of 0.951, and AUC of 0.998 with 200 trees. However, with a computationally more efficient model ($\sim$2 times faster than that of the same model with 200 tress) using 20 trees, we have obtained G-mean score of 0.9352 and F1 score of 0.9347 in discriminating the HRH patients from the LRH patients.

IV. CONCLUSION

In this study, we have proposed an automated prediction system to screen out the HRH patients. We have considered the issue of enormous missed/ectopic beats in such patients' data which could lead to a spurious HRV analysis, and presented a TVAR model based imputation technique to address the problem. The inadequacies of linear and CS interpolation technique in dealing with some kinds of outliers are demonstrated. We have conducted DTCWPT based time-frequency analysis of HRV signal for its robustness to shift invariance, besides its high frequency resolution and accordingly extracted features from it. Additionally, we study the characteristic of HRH patients' HRV based on statistical time domain indices and the complexity analysis using dispersion entropy under multiple scales to derive multiple features. Recognizing the class imbalance problem in the prediction/detection of such critical diseases, we check the performance of four different boosting algorithms to find the best classification model in reducing the false negative outcome. The proposed methodology provides G-mean score of 0.9352 and F1 score of 0.9347 with very low FNR of 3.37% and FPR of 1.56%. As an extension of this work, the efficacy of the system in detecting other critical cardiac diseases has to be assessed.

ACKNOWLEDGMENT

The authors would like to acknowledge Tezpur University for providing the necessary infrastructure to carry out this research.

REFERENCES

[1] (Sep. 13, 2019). *WHO Fact Sheets on Hypertension*. Accessed on: Feb. 2, 2021. [Online]. Available: https://www.who.int/news-room/fact-sheets/detail/hypertension

[2] A. Thomas, "Depression and vascular disease: What is the relationship?" *J. Affect. Disorders*, vol. 79, nos. 1–3, pp. 81–95, Apr. 2004.

[3] H. Mussalo, E. Vanninen, R. Ikäheimo, T. Laitinen, M. Laakso, E. Länsimies, and J. Hartikainen, "Heart rate variability and its determinants in patients with severe or mild essential hypertension," *Clin. Physiol.*, vol. 21, no. 5, pp. 594–604, Oct. 2008.

[4] G. K. Pal, P. Pal, N. Nanda, D. Amudharaj, and S. Karthik, "Spectral analysis of heart rate variability (HRV) may predict the future development of essential hypertension," *Med. Hypotheses*, vol. 72, no. 2, pp. 183–185, Feb. 2009.

[5] P. N. Casale, R. B. Devereux, M. Milner, G. Zullo, G. A. Harshfield, T. G. Pickering, and J. H. Laragh, "Value of echocardiographic measurement of left ventricular mass in predicting cardiovascular morbid events in hypertensive men," *Ann. Internal Med.*, vol. 105, no. 2, pp. 173–178, Aug. 1986.

[6] K. Nagai, S. Shibata, M. Akishita, N. Sudoh, T. Obara, K. Toba, and K. Kozaki, "Efficacy of combined use of three non-invasive atherosclerosis tests to predict vascular events in the elderly; carotid intima-media thickness, flow-mediated dilation of brachial artery and pulse wave velocity," *Atherosclerosis*, vol. 231, no. 2, pp. 365–370, Dec. 2013.

[7] A. E. Abbas, L. M. Franey, T. Marwick, M. T. Maeder, D. M. Kaye, A. P. Vlahos, W. Serra, K. Al-Azizi, N. B. Schiller, and S. J. Lester, "Noninvasive assessment of pulmonary vascular resistance by Doppler echocardiography," *J. Amer. Soc. Echocardiography*, vol. 26, no. 10, pp. 1170–1177, Oct. 2013.
[8] A. van Engelen, T. Wannarong, G. Parraga, W. J. Niessen, A. Fenster, J. D. Spence, and M. de Bruijne, "Three-dimensional carotid ultrasound plaque texture predicts vascular events," *Stroke*, vol. 45, no. 9, pp. 2695–2701, Sep. 2014.
[9] J. A. N. Dorresteijn, F. L. J. Visseren, A. M. J. Wassink, M. J. A. Gondrie, E. W. Steyerberg, P. M. Ridker, N. R. Cook, and Y. van der Graaf, "Development and validation of a prediction rule for recurrent vascular events based on a cohort study of patients with arterial disease: The SMART risk score," *Heart*, vol. 99, no. 12, pp. 866–872, Jun. 2013.
[10] P. Melillo, R. Izzo, A. Orrico, P. Scala, M. Attanasio, M. Mirra, N. D. Luca, and L. Pecchia, "Automatic prediction of cardiovascular and cerebrovascular events using heart rate variability analysis," *PLoS ONE*, vol. 10, no. 3, pp. 1–14, Mar. 2015.
[11] J. S. Rajput, M. Sharma, and U. R. Acharya, "Hypertension diagnosis index for discrimination of high-risk hypertension ECG signals using optimal orthogonal wavelet filter bank," *Int. J. Environ. Res. Public Health*, vol. 16, no. 21, p. 4068, Oct. 2019.
[12] D. C. K. Soh, E. Y. K. Ng, V. Jahmunah, S. L. Oh, T. R. San, and U. R. Acharya, "A computational intelligence tool for the detection of hypertension using empirical mode decomposition," *Comput. Biol. Med.*, vol. 118, pp. 1–6, Jan. 2020.
[13] K.-C. Lan, P. Raknim, W.-F. Kao, and J.-H. Huang, "Toward hypertension prediction based on PPG-derived HRV signals: A feasibility study," *J. Med. Syst.*, vol. 42, no. 6, pp. 1–7, Apr. 2018.
[14] M. Poddar, A. C. Birajdar, and J. Virmani, "Automated classification of hypertension and coronary artery disease patients by PNN, KNN, and SVM classifiers using HRV analysis," in *Machine Learning in Bio-Signal Analysis and Diagnostic Imaging*. Amsterdam, The Netherlands: Elsevier, 2019, pp. 99–125.
[15] T. H. Mäkikallio, H. V. Huikuri, A. Mäkikallio, L. B. Sourander, R. D. Mitrani, A. Castellanos, and R. J. Myerburg, "Prediction of sudden cardiac death by fractal analysis of heart rate variability in elderly subjects," *J. Amer. College Cardiol.*, vol. 37, no. 5, pp. 1395–1402, Apr. 2001.
[16] E. Ebrahimzadeh, M. Pooyan, and A. Bijar, "A novel approach to predict sudden cardiac death (SCD) using nonlinear and time-frequency analyses from HRV signals," *PLoS ONE*, vol. 9, no. 2, pp. 1–14, Feb. 2014.
[17] U. R. Acharya, H. Fujita, V. K. Sudarshan, D. N. Ghista, W. J. E. Lim, and J. E. W. Koh, "Automated prediction of sudden cardiac death risk using Kolmogorov complexity and recurrence quantification analysis features extracted from HRV signals," in *Proc. IEEE Int. Conf. Syst., Man, Cybern.*, Kowloon, China, Oct. 2015, pp. 1110–1115.
[18] R. Nicoll and M. Y. Henein, "Ginger (Zingiber officinale Roscoe): A hot remedy for cardiovascular disease?" *Int. J. Cardiol.*, vol. 131, no. 3, pp. 408–409, Jan. 2009.
[19] A. Sajadieh, V. Rasmussen, H. O. Hein, and J. F. Hansen, "Familial predisposition to premature heart attack and reduced heart rate variability," *Amer. J. Cardiol.*, vol. 92, no. 2, pp. 234–236, Jul. 2003.
[20] Z. Binici, M. R. Mouridsen, L. Køber, and A. Sajadieh, "Decreased nighttime heart rate variability is associated with increased stroke risk," *Stroke*, vol. 42, no. 11, pp. 3196–3201, Nov. 2011.
[21] A. Kampouraki, G. Manis, and C. Nikou, "Heartbeat time series classification with support vector machines," *IEEE Trans. Inf. Technol. Biomed.*, vol. 13, no. 4, pp. 512–518, Jul. 2009.
[22] A. L. Goldberger, L. A. N. Amaral, L. Glass, J. M. Hausdorff, P. C. Ivanov, R. G. Mark, J. E. Mietus, G. B. Moody, C.-K. Peng, and H. E. Stanley, "PhysioBank, PhysioToolkit, and PhysioNet: Components of a new research resource for complex physiologic signals," *Circulation*, vol. 101, no. 23, pp. e215–e220, Jun. 2000.
[23] A. M. Bianchi, L. Mainardi, E. Petrucci, M. G. Signorini, M. Mainardi, and S. Cerutti, "Time-variant power spectrum analysis for the detection of transient episodes in HRV signal," *IEEE Trans. Biomed. Eng.*, vol. 40, no. 2, pp. 136–144, Feb. 1993.
[24] H. Akaike, "A new look at the statistical model identification," *IEEE Trans. Autom. Control*, vol. AC-19, no. 6, pp. 716–723, Dec. 1974.
[25] R. M. Rangayyan, *Biomedical Signal Analysis: A Case-Study Approach*, 2nd ed. Hoboken, NJ, USA: Wiley, 2015, pp. 499–507.
[26] M. Malik, "Heart rate variability: Standards of measurement, physiological interpretation, and clinical use: Task force of the European society of cardiology and the North American society for pacing and electrophysiology," *Ann. Noninvasive Electrocardiol.*, vol. 1, no. 2, pp. 151–181, Apr. 1996.
[27] D. Deka and B. Deka, "Characterization of heart rate variability signal for distinction of meditative and pre-meditative states," *Biomed. Signal Process. Control*, vol. 66, Apr. 2021, Art. no. 102414.
[28] B. Hjorth, "EEG analysis based on time domain properties," *Electroencephalogr. Clin. Neurophysiol.*, vol. 29, no. 3, pp. 306–310, Sep. 1970.
[29] I. Bayram and I. W. Selesnick, "On the dual-tree complex wavelet packet and M-band transforms," *IEEE Trans. Signal Process.*, vol. 56, no. 6, pp. 2298–2310, Jun. 2008.
[30] M. Costa, A. L. Goldberger, and C.-K. Peng, "Multiscale entropy analysis of complex physiologic time series," *Phys. Rev. Lett.*, vol. 89, no. 6, Jul. 2002, Art. no. 068102.
[31] M. Rostaghi and H. Azami, "Dispersion entropy: A measure for time-series analysis," *IEEE Signal Process. Lett.*, vol. 23, no. 5, pp. 610–614, May 2016.
[32] H. Peng, F. Long, and C. Ding, "Feature selection based on mutual information criteria of max-dependency, max-relevance, and min-redundancy," *IEEE Trans. Pattern Anal. Mach. Intell.*, vol. 27, no. 8, pp. 1226–1238, Aug. 2005.
[33] C. Seiffert, T. M. Khoshgoftaar, J. Van Hulse, and A. Napolitano, "RUSBoost: A hybrid approach to alleviating class imbalance," *IEEE Trans. Syst., Man, Cybern., A, Syst. Humans*, vol. 40, no. 1, pp. 185–197, Jan. 2010.
[34] N. V. Chawla, A. Lazarevic, L. O. Hall, and K. W. Bowyer, "SMOTEBoost: Improving prediction of the minority class in boosting," in *Knowledge Discovery in Databases: PKDD* (Lecture Notes in Computer Science), vol. 2838. Berlin, Germany: Springer, 2003, pp. 107–119.
[35] N. Nikolaou, N. Edakunni, M. Kull, P. Flach, and G. Brown, "Cost-sensitive boosting algorithms: Do we really need them?" *Mach. Learn.*, vol. 104, nos. 2–3, pp. 359–384, Aug. 2016.
[36] Y. Sun, A. K. C. Wong, and Y. Wang, "Parameter inference of cost-sensitive boosting algorithms," in *Machine Learning and Data Mining in Pattern Recognition*. (Lecture Notes in Computer Science), vol. 3587. Berlin, Germany: Springer, 2005, pp. 21–30.

DIPEN DEKA (Member, IEEE) received the B.E. degree in instrumentation engineering from Assam Engineering College, in 2005, and the M.Tech. degree in electronics and communication technology from Gauhati University, India, in 2013. He is currently pursuing the Ph.D. degree with the Department of Electronics and Communication Engineering, Tezpur University, India. He is currently an Assistant Professor with the Department of Instrumentation Engineering, Central Institute of Technology (CIT) Kokrajhar, India. His research interests include biomedical signal processing, transducer and signal conditioning, and embedded systems.

BHABESH DEKA (Senior Member, IEEE) received the B.E. degree in electronics and telecommunication engineering from Assam Engineering College, in 1999, the M.Tech. degree in electronics design and technology from Tezpur University, Assam, India, in 2001, and the Ph.D. degree in image processing from IIT Guwahati, in 2011.

He is currently a Professor with the Department of Electronics and Communication Engineering, Tezpur University. He has authored Springer book series on *Bio- and Neurosystems*, among several other international publications. He is a fellow of the Institution of Electronics and Telecommunication Engineers (IETE). His major research interests include image processing, computer vision and machine learning for biomedical signal/image analysis.